

## Influence of post annealing temperature on the thermoelectric properties of bulk ZnSnO

H. T. Ali<sup>a</sup>, U. Rehman<sup>b</sup>, K. Mahmood<sup>b,\*</sup>, M. Yusuf<sup>c</sup>, S. Ikram<sup>b</sup>, A. Ali<sup>b</sup>, N. Amin<sup>b</sup>, A. Ashfaq<sup>b</sup>, Y. Ali<sup>b</sup>, M. A. Sajjad<sup>d</sup>

<sup>a</sup>Department of Mechanical Engineering, College of Engineering, Taif University, P.O. Box 11099, Taif 21944, Saudi Arabia

<sup>b</sup>Department of Physics, Government College University Faisalabad, Pakistan

<sup>c</sup>Department of Clinical Pharmacy, College of Pharmacy, Taif University, P.O. Box 11099, Taif 21944, Saudi Arabia

<sup>d</sup>Department of Chemistry, Division of Science and Technology, University of Education Lahore, Pakistan

In this manuscript, we have studied the structural, electrical and thermoelectric properties of bulk ZnSnO by post growth annealing method. X-Ray Diffraction data showed that the crystallinity was found to be improved by annealing up to 700°C due to compensation of oxygen vacancy type donor defects. But further annealing forced the oxygen atoms to diffuse into the interstitial sites, therefore causes degradation in the crystal quality. Thermoelectric properties were increased with annealing temperature up to 700°C and then decreased due to further annealing. The sharp enhancement of thermoelectric properties is due to mobility increase of carriers.

(Received April 14, 2021; Accepted July 23, 2021)

*Keywords:* ZnSnO, XRD, SEM, Seebeck effect, Power factor

### 1. Introduction

With the growing world energy demands, limited conventional energy resources and emission of greenhouse gases are threatening to our environment. More than 80% of world energy is obtained by fossil fuel with more than half of this energy is wasted in the form of heat. As the world energy consumption continues to rise, so the shifting toward renewable energy resources like windmill, solar energy, hydroelectric, thermo-electric devices and fuel cells is necessary [1-4]. Thermo-electric materials are the hot topic for the researchers nowadays because of their excellent energy harvesting properties i.e. Electricity generation from the waste heat by using the phenomenon of the Seebeck effect [5]. Beside this it has some advantages like noise free, no mechanical or moving part, maintenance free, cost effective and long-life applications [6,7]. The efficiency of any thermo-electric device can be defined by a dimensionless quantity called a figure of merit (ZT) which is termed as [8]

$$ZT = S^2T / \rho K$$

All quantities have usual meaning. The conversion efficiency of any thermoelectric device increases with increasing the Seebeck coefficient or by lowering the electrical resistivity and thermal conductivity. Telluride based materials e.g. BiTe and PbTe and their alloys are widely used as commercial thermoelectric materials due to their high conversion rate [9, 10]. However, the high manufacturing cost limits its application for large scale energy production. In contrast, ZnO and its variants are emerging as an excellent thermoelectric material with the remarkable electrical, optical and thermoelectric properties [11]. Beside this ZnO with a wide band gap (3.3 eV), n-type conductivity and high temperature suitability makes it a potential candidate for high temperature

---

\* Corresponding author: Khalid\_mahmood856@yahoo.com

thermoelectric applications [12]. So, the doping or alloying of ZnO with another element might enhance its thermoelectric properties [13-17]. Sn is supposed to be a strong doping element in ZnO and easy to replace zinc because it has comparable atomic radii. However, Sn doping in ZnO can significantly enhance the Seebeck coefficient and electrical conductivity hence increase in power factor as reported in the literature so far [18, 19].

In this paper, we have reported the modulation in the thermoelectric properties of bulk ZnSnO by varying the post annealing temperature. The ZnSnO pellets were prepared by mixing of ZnO and Sn powders using a hydraulic press at a pressure of 13 tons. The prepared pellets were subjected to post annealing process at different annealing temperature from 500 to 800°C. XRD data confirm that the sample annealed at 700°C shows best crystallinity and have the highest value of Seebeck coefficient and power factor.

## 2. Experimental detail

ZnSnO based bulk composites were prepared by mixing 99% pure ZnO and Sn metal powders obtained from Sigma Aldrich. Both powders were mixed by using 98% ZnO and 2% Sn by keeping the net weight about 0.45g for each pellet. Agate mortar and pestle were used for the mixing of powders while a very small amount of acetone was added during the grinding process to improve the homogeneity of the mixture for 2hours. After that ZnSnO pellets were prepared by using a hydraulic press at a pressure of 13 ton for 30 minutes. The prepared pellets were subjected to post annealing process at different annealing temperature from 500°C to 800°C with step of 100°C in programmable muffle furnace for 1 hour.

The post annealed bulk ZnSnO samples were characterized by X-ray diffraction (Bruker D8 advanced) to study structural properties and Raman spectroscopy (Dongwoo confocal micro Raman mapping system) were used to study the vibrational and rotational modes of the samples. Scanning electron microscope (Emcrafts Cube series) was used to evaluate the surface morphology. For thermoelectric properties home developed Seebeck systems were used while the Hall measurement (Ecopia 3000) was performed to measure the electrical conductivity.

## 3. Results and discussion

Figure1 (a) shows the XRD pattern of ZnSnO samples at various post annealing temperature from 500 to 800°C at step of 100°C for 60 minutes. The peaks observed at angle  $2\theta = 32.2^\circ, 34.9^\circ, 36.6^\circ, 47.9^\circ, 56.9^\circ, 63.2^\circ, 66.7^\circ, 68.3^\circ, 69.4^\circ, 77.3^\circ$  is associated to the hexagonal structure of Sn doped ZnO with miller indices (100), (002), (101), (102), (110), (103), (200), (112), (201) and (202) respectively [20]. No additional secondary peak related to SnO or SnO<sub>2</sub> is observed. It is observed that as the post annealing temperature is increased, the crystallinity of the samples increases up to 700°C and then decreases with further rise in annealing temperature. It is accepted fact that ZnO has a large number of oxygen vacancy intrinsic defects so annealing in an oxygen environment compensate the such defects because additional incoming oxygen atoms fill the available oxygen vacancies and hence improvement in crystallinity [21]. But annealing at 800°C additional upcoming oxygen atom occupying the interstitial sites cause degradation in crystallinity.

Figure1 (b) also represent the Raman spectra of the ZnSnO sample at different post annealing temperature from 500 to 800°C. A very sharp peak at  $437\text{cm}^{-1}$  is observed in all the samples which is related to the E<sub>g</sub> mode of ZTO [23]. A large hump at  $328\text{cm}^{-1}$  and  $378\text{cm}^{-1}$  was observed, which can be attributed to A<sub>1</sub> (TO) and  $E_2^{\text{high}} - E_2^{\text{low}}$  non-polar modes of ZnO [24, 25]. While the peak at  $587\text{cm}^{-1}$  is assigned as and E<sub>1</sub> (LO) mode of ZnO respectively. A small peak around  $540\text{cm}^{-1}$  is appeared for the post annealed samples which can be related as A<sub>2u</sub> (TO) mode of SnO<sub>2</sub> [26]. The presence of Sn confirms the diffusion of Sn content in the ZnO matrices. The highest intensity peak at  $437\text{cm}^{-1}$  shows an increasing trend with the annealing temperature up

to 700°C and again decreasing with the further increase in annealing temperature having same trend as XRD data.

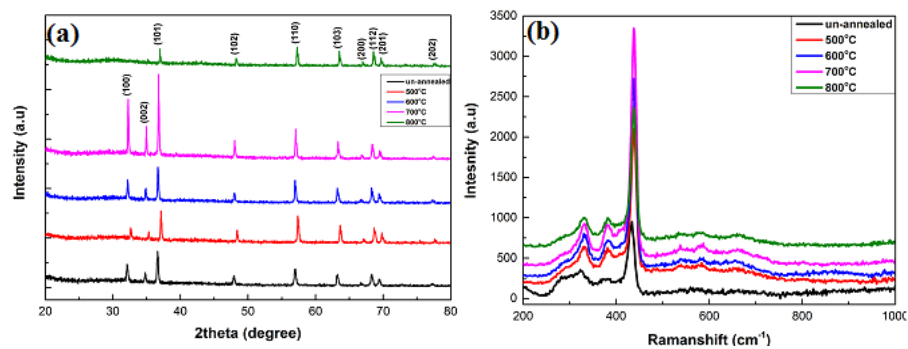


Fig. 1. (a) XRD and (b) Raman spectrum of ZnSnO pellets post annealed at different temperatures ranges from 500-800°C.

Figure 2 represents the surface morphology of the ZnSnO samples at different post annealing temperature. In fig (2a) the un-annealed sample shows a fine, smooth morphology, but with post annealing from 500 to 800°C the surface of the samples exhibits rough morphology fig (2b) -(2e). It is also observed that the roughness of the samples goes on increasing with increase in post annealing temperature, which can be related to the incoming oxygen atoms give rise to degradation of the surface.

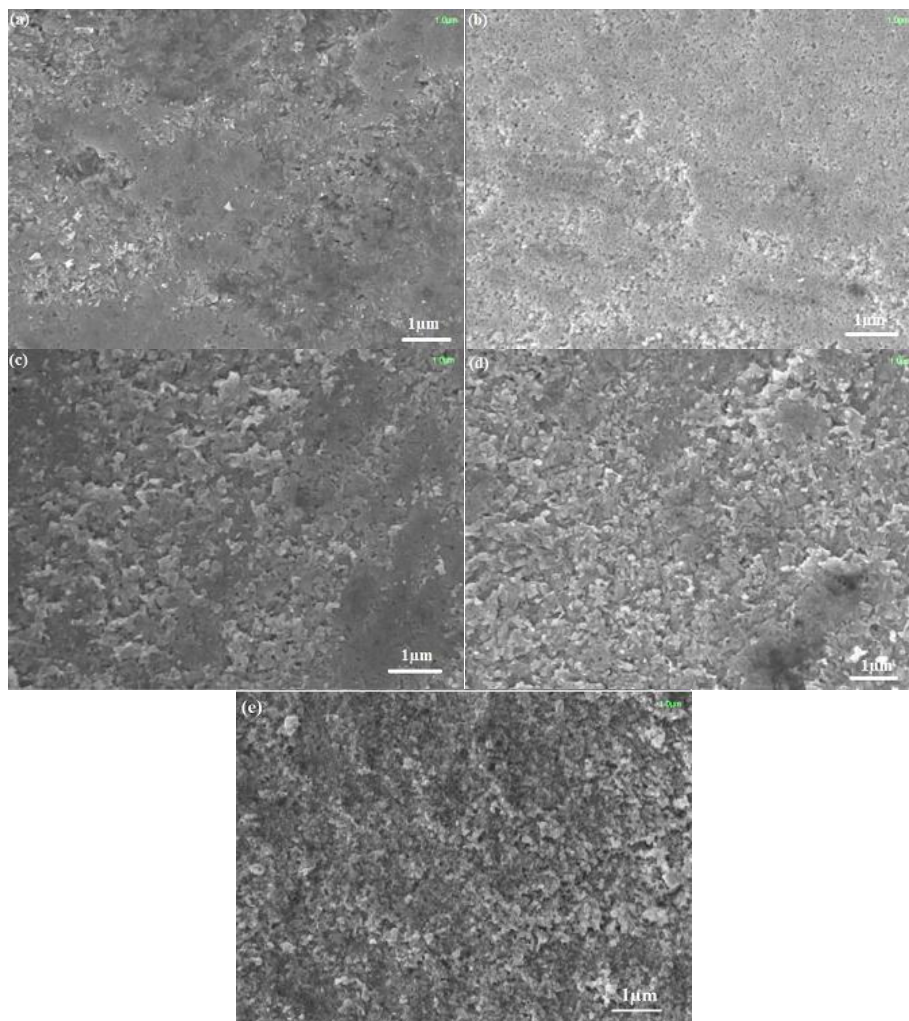


Fig. 2. SEM images of ZnSnO pallets annealed at different temperatures ranges from 500-800°C.

Figure3 depicts the Seebeck coefficient versus annealing temperature of the samples, post annealed at different annealing temperature from 500 to 800°C. The value of the Seebeck coefficient shows an increasing trend with the increase in post annealing temperature up to 700°C and again decreasing with the further rise in temperature. The negative value of Seebeck coefficient is observed for all of the samples shows n-type behavior of the material. The increase in Seebeck coefficient up to 700°C is related to the solubility of Sn atoms in the ZnO crystal due to thermal annealing which is debatable. The enhancement in Seebeck coefficient from 500 to 700°C is due to fact that most of the available oxygen vacancies filled by incoming atoms and causes an enhancement in the mobility of charge carriers. The high mobility resulted in the enhancement of Seebeck coefficient and electrical conductivity. But the further rise in annealing temperature cause degradation in the crystal quality hence decrease in Seebeck coefficient is expected.

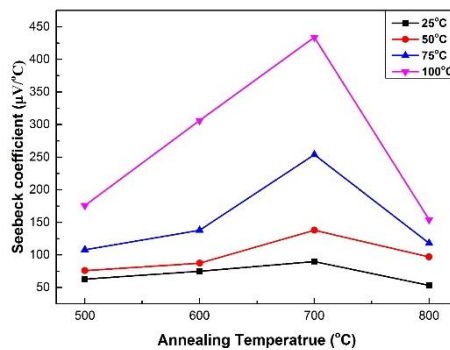


Fig. 3. Effect of annealing temperature on Seebeck coefficient of ZnSnO pallets at different measurement temperature.

Figure4 represent the effect of post annealing temperature on the electrical conductivity of the ZnSnO samples.

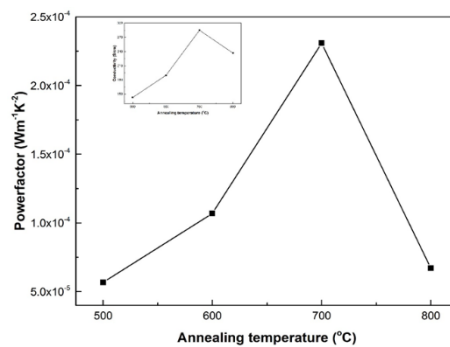


Fig. 4. The graph represents the effect of annealing temperature on the power factor of ZnSnO pallets. The inset demonstrates the effect of annealing temperature on the electrical conductivity of the ZnSnO samples.

The value of electrical conductivity shows an increasing trend up to 700°C and again decrease at 800°C. The behavior of electrical conductivity with post annealing temperature is attributed as; the mobility of carriers increased with the annealing temperature because the scattering of charge carriers by the oxygen vacancy type defects decreased up to annealing

temperature 700°C. But at high annealing temperature the conduction mechanism is shifted from lattice to ionized impurity scattering mechanism cause decrease in mobility and hence decrease in electrical conductivity is observed. The power factor of the ZnSnO samples which is calculated by using this formula [27].

$$P.F = S^2 \times \sigma$$

As the sample annealed at 700°C possess the highest value of Seebeck coefficient and electrical conductivity so the highest power factor value at 700°C is justified.

### 3. Conclusion

In this manuscript we have reported the effect of post annealing temperature on the thermoelectric properties of ZnSnO pellets using Sn and ZnO powders. The pellets were prepared by using a hydraulic press at a pressure of 13 tons and the post annealed at different annealing temperature ranges from 500°C to 800°C at step of 100°C for 1 hour. XRD data reveal that 700°C samples show best crystallinity and possess the highest value of Seebeck coefficient, electrical conductivity and power factor. SEM images show higher surface roughness of the sample annealed at 800°C. So, this study reveals that the sample annealed at 700°C can be used for high temperature thermoelectric applications.

### Acknowledgements

The current research is supported by Taif University Researchers Supporting Project Number (TURSP-2020/293), Taif University, Taif, Saudi Arabia.

### References

- [1] R. Zahra, K. Mahmood, A. Ali, U. Rehman, N. Amin, M. I. Arshad, S. Hussain, M. H. Mahmood, *Ceramics International* **45**, 312 (2019).
- [2] R. Zahra, J. Jacob, N. Bano, A. Ali, K. Mahmood, S. Ikram, M. I. Arshad, A. Ashfaq, U. Rehman, S. Hussain, *Physica B: Condensed Matter* **564**, 143 (2019).
- [3] A. Ali, J. Jacob, A. Ashfaq, M. Tamseel, K. Mahmood, N. Amin, S. Hussain, W. Ahmad, U. Rehman, S. Ikram, D. S. Al-Othmany, *Ceramics International* **45**, 12820 (2019).
- [4] J. Jacob, R. Wahid, A. Ali, R. Zahra, S. Ikram, N. Amin, A. Ashfa, U. Rehman, S. Hussain, D. S. Al-Othmany, S. Z. Ilyas, *Physica B: Condensed Matter* **562**, 59 (2019).
- [5] K. Mahmood, S. Abbasi, R. Zahra, U. Rehman, *Ceramics International* **44**, 17905 (2018).
- [6] J. Jacob, K. Mahmood, M. Y. Usman, U. Rehman, A. Ali, A. Ashfaq, N. Amin, S. Ikram, S. Hussain, *Physica B: Condensed Matter* **572**, 247 (2019).
- [7] K. Mahmood, J. Jacob, A. Rehman, A. Ali, U. Rehman, N. Amin, S. Ikram, A. Ashfaq, S. Hussain, *Ceramics International* **45**, 18701 (2019).
- [8] K. Tian, A. Tiwari, *Scientific reports* **9**, 3133 (2019).
- [9] K. Kim, G. Kim, H. Lee, K. H. Lee, W. Lee, *Scripta Materialia* **145**, 41 (2018).
- [10] C. Han, G. Tan, T. Varghese, M. G. Kanatzidis, Y. Zhang, *ACS Energy Letters* **3**, 818 (2018).
- [11] J. Kennedy, P. P. Murmu, J. Leveneur, V. M. Williams, R. L. Moody, T. Maity, S. V. Chong, *Journal of nanoscience and nanotechnology* **18**, 1384 (2018).
- [12] K. V. Zakharchuk, D. M. Tobaldi, X. Xiao, W. Xie, S. M. Mikhalev, J. F. Martins, J. R. Frade, A. Weidenkaff, A. V. Kovalevsky, *Journal of the European Ceramic Society* **39**, 1222 (2019).
- [13] Q. Zhang, G. Xia, L. Li, W. Xia, H. Gong, S. Wang, *Current Applied Physics* **19**, 174 (2019).
- [14] M. M. Jumidali, K. M. Sulieman, M. R. Hashim, *Appl. Surf. Sci.* **257**, 4890 (2011).

- [15] M. Ullah, W.B. Su, A. Manan, A.S. Ahmad, A.A. Shah, Z. Yao, *Phase, Ceram. Int.* **44**, 17873 (2018).
- [16] T. M. V. M. Thiruvalluvan, V. Natarajan, V. Manimuthu, S. Valanarasu, P. Anandan, M. Arivanandhan, *J. Phys. Chem. Solids* **122**, 162 (2018).
- [17] G. Li, X. Lin, S. Liu, B. Jia, Q. Wang, *Appl. Surf. Sci.* **439**, 82 (2018).
- [18] U. Rehman, J. Jacob, K. Mahmood, A. Ali, A. Ashfaq, N. Amin, S. Ikram, W. Ahmad, S. Hussain, *Physica B: Condensed Matter* **570**, 232 (2019).
- [19] W. Guan, L. Zhang, C. Wang, Y. Wang, *Y. Materials Science in Semiconductor Processing* **66**, 247 (2017).
- [20] P. Nunes, E. Fortunato, P. Tonello, F. B. Fernandes, P. Vilarinho, R. Martins, *Vacuum* **64**, 281 (2002).
- [21] L. Lin, J. Liu, J. Lv, S. Shen, X. Wu, D. Wu, Y. Qu, W. Zheng, F. Lai, *J. Alloy. Compd.* **695**, 1523 (2017).
- [22] M. Asghar, K. Mahmood, M.-A. Hasan, *Key Eng. Mater.* **510**, 132 (2012).
- [23] S. Horzum, F. Iyikanat, R. T. Senger, C. Çelebi, M. Sbeta, A. Yildiz, T. Serin, *Journal of Molecular Structure* **1180**, 505 (2019).
- [24] R. A. Mereu, A. Le Donne, S. Trabattoni, M. Acciarri, S. Binetti, *Journal of Alloys and Compounds* **626**, 112 (2015).
- [25] R. Cuscó, E. Alarcón-Lladó, J. Ibáñez, L. Artús, J. Jiménez, B. Wang, M. J. Callahan, *Physical Review B* **75**, 165202 (2007).
- [26] C. S. Ferreira, P. L. Santos, J. A. Bonacin, R. R. Passos, L. A. Pocrifka, *Materials Research* **18**, 639 (2015).
- [27] A. Rehman, J. Jacob, R. Zahra, K. Mahmood, A. Ali, U. Rehaman, Y. Ali, A. Ashfaq, W. Ahmad, S. Ikram, N. Amin, S. Hussain, *Ceramics International* **45**, 16275 (2019).